Chapter 4

Improved Amber and Opal Suppressor tRNAs for Incorporation of Unnatural Amino Acids *In Vivo*, Part 1. Minimizing Misacylation of Suppressor tRNAs.

This chapter is reproduced, with modification, from *Improved amber and opal suppressor tRNAs for incorporation of unnatural amino acids in vivo. Part 1: Minimizing misacylation*, by E. A. Rodriguez, H. A. Lester, and D. A. Dougherty, (2007) *RNA*, **13(10)**, 1703–1714.

4.1 Introduction

Incorporation of unnatural amino acids (UAAs) site-specifically in proteins biosynthetically is a powerful tool that is increasingly being used. The primary approach has been stop codon (nonsense) suppression using a designed tRNA with an anticodon recognizing the stop codon. In higher eukaryotes, nonsense suppression by a tRNA chemically aminoacylated with an UAA (tRNA-UAA) is primarily limited to *Xenopus* oocytes, where microinjection of the mutant mRNA and tRNA-UAA is straightforward, and electrophysiology allows for sensitive detection of UAA incorporation (shown in Figure 3.1) (1,2). Recently, site-specific UAA incorporation was performed in *Xenopus* oocytes using frameshift suppression of the quadruplet codons CGGG and GGGU, which allowed for the simultaneous incorporation of three UAAs (3).

THG73, an amber suppressor tRNA from *T. thermophila* with a G73 mutation, has been used extensively to incorporate over 100 residues in 20 different proteins (1,2). With THG73 and any other suppressor tRNAs, a key issue is orthogonality. An orthogonal tRNA is one that is not measurably aminoacylated with natural amino acids (aas) by endogenous aminoacyl-tRNA synthetases (aaRSs). Unlike its mathematical counterpart, there can be degrees of orthogonality when referring to tRNAs. While the orthogonality of THG73 has been evaluated using *in vitro* translation in *E. coli* (4), wheat germ (5), and rabbit reticulocyte lysate (6), the primary application of THG73 has been for *in vivo* translation in *Xenopus* oocytes, which is the focus of the present work. The orthogonality of THG73 is acceptable when injecting low quantities of mutant

mRNA and/or tRNA-UAA with incubation times less than 2 d (7,8). However, increasing the amount of mutant mRNA and/or tRNA-UAA, or incubation times of 2 d — which we will term "excessive" conditions — led to increased aminoacylation of THG73 *in vivo* with natural aa(s) (3). This is highly undesirable, because incorporation of natural aas at the suppression site leads to a heterogeneous mixture of proteins containing an UAA or natural aa(s) and limits the quantity of protein that can be produced by UAA incorporation.

Previous work from our labs showed that yeast Phe frameshift suppressor tRNAs ($YFFS_{CCCG}$ and $YFaFS_{ACCC}$) were aminoacylated much less than THG73 *in vivo*, but suppression of the quadruplet codons was less efficient than with THG73 and varied greatly with the amount of frameshift suppressor tRNA injected (3). Previously, an *E. coli* Asn amber suppressor (ENAS) tRNA was shown to be highly orthogonal *in vivo* (9) and *in vitro* (4,10,11). Here we show that ENAS has similar amounts of aminoacylation to THG73, suggesting that other well-characterized amber suppressor tRNAs could be prone to aminoacylation under excessive conditions.

Therefore, we chose to determine the aa that was being placed on THG73 using the sensitivity of electrophysiology and a well-characterized mutation site of the nicotinic acetylcholine receptor (nAChR), and determined the aa to be Gln. Using this knowledge, we created "Knob" mutations on THG73 previously shown to reduce aminoacylation of *E. coli* $tRNA_2^{Gln}$ by the *E. coli* glutaminyl-tRNA synthetase (GlnRS) (12). The Knob mutations on THG73 resulted in tRNAs that showed drastically reduced

suppression efficiency *in vivo*, making them not viable replacements. The *E. coli* GlnRS has been shown to interact with the acceptor stem of the tRNA in the crystal structure (13), which was subsequently shown to be sensitive to base pairs and/or backbone positioning of the tRNA acceptor stem (14–16). We created seven unique tRNAs with mutations in the 2nd to 4th positions of the acceptor stem, and analyzed their function *in vivo* relative to THG73. Mutations in the acceptor stem decreased aminoacylation significantly. This library of *T. thermophila* Gln amber suppressor (TQAS) tRNAs can be used to screen for orthogonality in other eukaryotic cells. To show the generality of the acceptor stem mutations, we also created *T. thermophila* Gln opal suppressor (TQOpS' and TQOpS) tRNAs that are also aminoacylated less than THG73. The acceptor stem mutations have general application for the creation of orthogonal suppressor tRNAs for UAA incorporation in higher eukaryotic cells, where random mutagenesis combined with high-throughput screens is not readily applicable.

4.2 Results

4.2.1 Schematic for Site-Specific UAA Incorporation and Aminoacylation

Figure 4.1 shows a schematic for the steps leading to UAA incorporation *in vivo*. Upon injection of the tRNA-dCA-UAA, the tRNA can bind to EF-1α and/or other components of the translational machinery in a reversible fashion (Figure 4.1, A). It has been shown that the prokaryotic ortholog EF-Tu can protect tRNA-dCA-UAA from hydrolysis *in vitro* (17) (Figure 4.1, C), thus favoring incorporation of UAA by

recognition of the suppressor site on the mRNA (Figure 4.1, B). If tRNA lacking the terminal CA (74mer) is injected, it can be converted to the full-length tRNA by the addition of CA *in vivo* (Figure 4.1, D). The full-length tRNA, either tRNA-dCA or tRNA-CA (76mer), may then be aminoacylated with a natural aa by an endogenous aaRS (Figure 4.1, E). The tRNA-dCA-aa can then bind EF-1α and/or other components of the translational machinery (Figure 4.1, F) and lead to the incorporation of a natural aa at the suppression site (Figure 4.1, G) in competition with the suppression by tRNA-dCA-UAA (Figure 4.1, B), a highly undesirable outcome. After translation, both UAA and natural aa incorporation causes the tRNA-dCA/CA to be released from the ribosome (Figure 4.1, H), which can further contribute to the undesired natural aa incorporation (Figure 4.1, E–G).

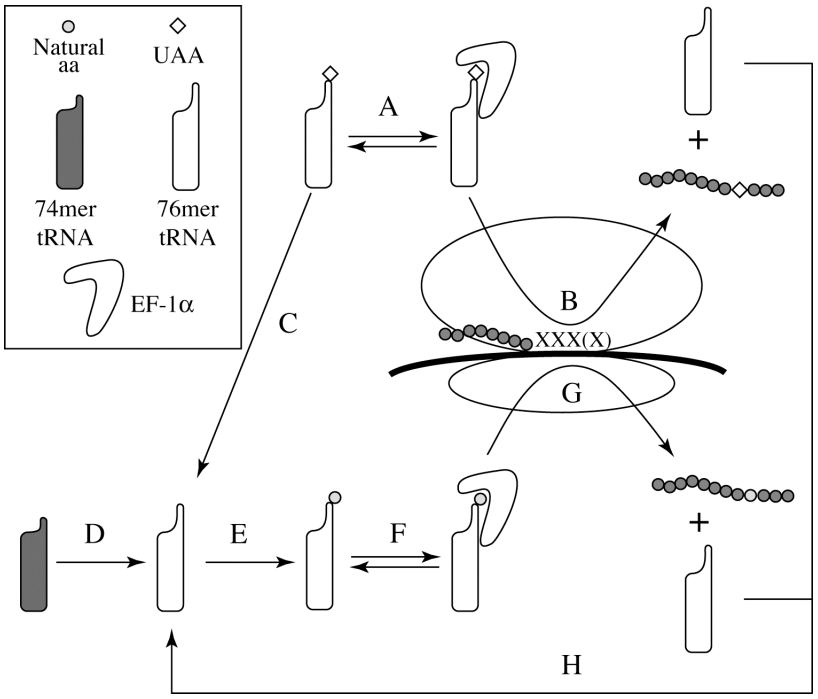

Figure 4.1: Site-specific UAA incorporation. (A) tRNA-dCA-UAA binds EF-1α and/or other components of the translational machinery. (B) UAA is incorporated at the suppression site (XXX(X)), resulting in a protein with an UAA. (C) Undesired hydrolysis and/or aaRS editing results in irreversible loss of the UAA, resulting in tRNA-dCA (76mer). (D) Injection of the tRNA (lacking dCA, 74mer) is converted to a 76mer *in vivo* by the addition of CA (tRNA-CA). (E) Undesired recognition of the suppressor tRNA-dCA/CA by endogenous aaRS(s) can result in aminoacylation of the tRNA with a natural aa. (F) tRNA-dCA/CA-aa binds EF-1α and/or other components of the translational machinery. (G) Undesired protein translation can occur by placing a natural aa at the suppressor site (XXX(X)), rather then termination at the stop codon or a frameshift, and this competes with UAA incorporation. (H) After translation the tRNA-dCA/CA is released into the cytoplasm and can repeat steps E–H.

4.2.2 Experimental Scheme for Evaluating Aminoacylation and Suppression by Electrophysiology

All experiments were performed on the nAChR, which has been extensively studied by the site-specific incorporation of UAAs. The muscle-type nAChR is a pentamer composed of α-, β-, γ-, and δ-subunits in the ratio of 2:1:1:1, respectively

(Figure 3.3). In order to compare experiments from different batches of oocytes, we normalized the average maximal current in response to 1 mM ACh for each suppressor tRNA to the corresponding average maximal current for THG73. Wild-type mRNA expression would be the most desirable normalization, but injection of 20–60 ng of mRNA (as in the aminoacylation experiments) would produce wild-type currents greater than 100 μA, resulting in current saturation.

To evaluate aminoacylation, we chose a Leu site in the second transmembrane helix (M2) of the β subunit termed β9' (shown in Figure 3.3). This site has been shown to tolerate placement of many natural aas and UAAs (18–20), with most causing characteristic shifts in ACh EC_{50}. Previously, THG73 was shown to incorporate natural aa(s) at this site under excessive conditions (3). A possible complication for experiments designed to probe aminoacylation is read-through of the stop codon, which can be tested for by injecting mRNA only into the *Xenopus* oocyte. We find that at the β9' site, such read-through is insubstantial, producing currents that are ≈ 3.5% of those seen when THG73 is included.

During the course of this research, we noticed variations in aminoacylation depending on whether the oocytes were acquired from Xenopus Express or Nasco. *Xenopus laevis* frogs from Xenopus Express are caught in Africa, while Nasco frogs are bred in a laboratory and are from a similar gene pool (Linda Northey, personal communication). For each experiment, the figure legends state the supplier(s) of the oocytes.

4.2.3 Identifying the Natural aa Placed on THG73 Using Electrophysiology

As noted above, we focus on the β9' site of the nAChR, which for the wild-type β9'L (shown in Figure 3.3) has an EC_{50} of 50 μM for ACh. For the well-characterized β9'S the EC_{50} is lowered ≈ 33-fold to 1.5 μM ACh (18), and the lowering of EC_{50} has been shown to scale with the polarity of the residue introduced at the β9' position (18).

Injection of β9'UAG + THG73 (74mer) under excessive conditions produces receptors with an EC_{50} of 0.24 μM ACh (Figure 4.2), which is lower than any substitution previously tested at the β9' position. When β9'UAG + THG73-dCA (76mer) was evaluated, an EC_{50} of 0.88 μM was obtained. We chose to screen β9'Q because THG73 evolved to suppress the amber codon with Gln in *T. thermophila* (21), and many amber suppressor tRNAs are aminoacylated with Gln *in vivo* (22). The conventional mutant β9'Q has an EC_{50} of 0.31 μM ACh (Figure 4.2). While the EC_{50} of β9'Q and β9'UAG + THG73 (74mer) are comparable, there is ≈ 3-fold increase in EC_{50} when β9'UAG + THG73-dCA (76mer) is injected (Figure 4.2). These results suggest that the full-length THG73-dCA (76mer) is aminoacylated with amino acids other than Gln. Apparently, this is less important for THG73 (74mer), which must have CA added *in vivo* to become a full-length tRNA (Figure 4.1, D). From these results, we conclude that the predominant natural aa placed on THG73 is Gln.

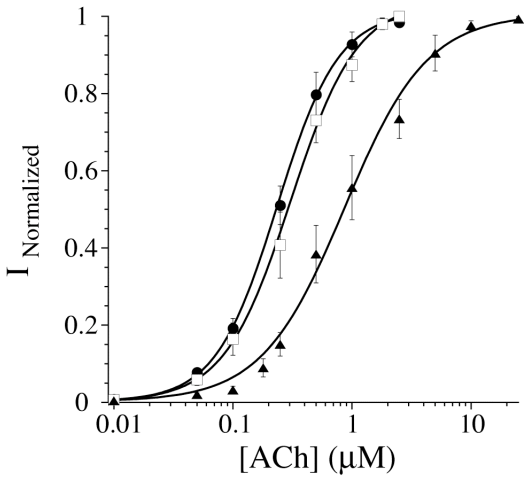

Figure 4.2: Fits to the hill equation for β9'UAG + THG73 (74mer)/-dCA (76mer) and β9'Q. Filled circles are β9'UAG + THG73 (74mer) [16 ng per oocyte], open squares are β9'Q, and filled triangles are β9'UAG + THG73-dCA (76mer) [5 ng per oocyte]. EC_{50} values are .24 ± .006, .31 ± .02, and .88 ± .08 μM ACh, respectively. In each experiment $n > 3$ oocytes.

4.2.4 Testing Knob Mutations on THG73

Much is known about the recognition of tRNA by the GlnRS, and key interactions have been assigned to various "knobs" on the tRNA, termed K1, K2, and K3 (Figure 4.3). In a study of aminoacylation of *E. coli* $tRNA_2^{Gln}$ by the *E. coli* GlnRS (12), the mutations that produced the greatest reduction in aminoacylation were K2, K2K3, and K1K2K3. We therefore incorporated these mutations into THG73, and tested for orthogonality at the β9' site.

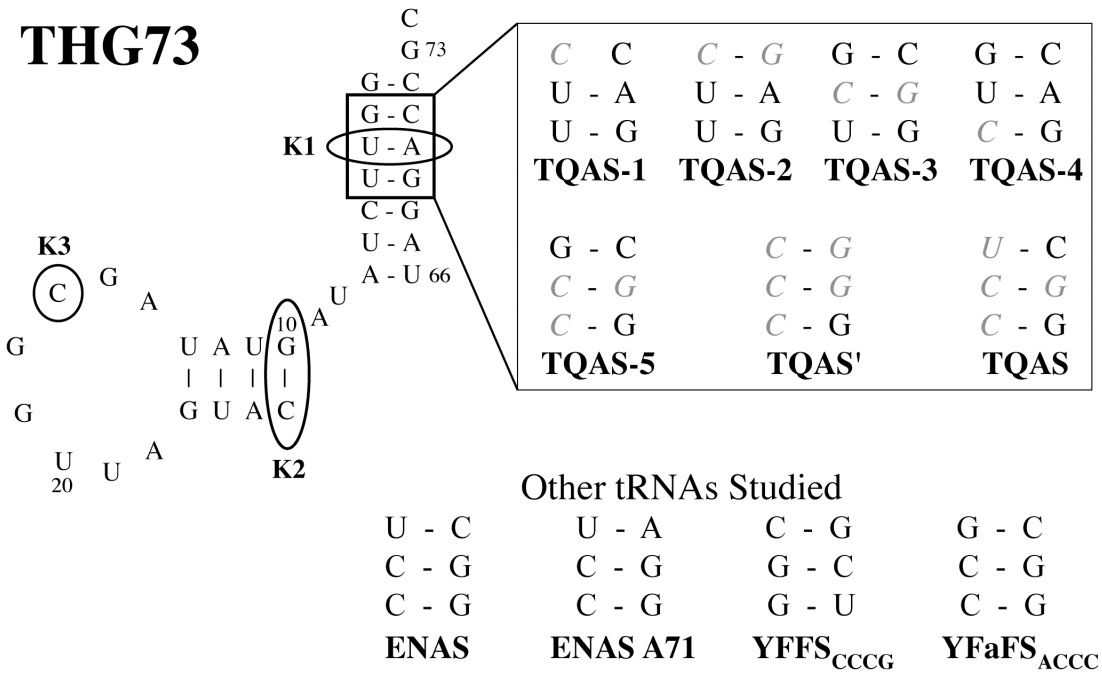

Figure 4.3: THG73 mutations and tRNAs studied. Circled positions on THG73 correspond to the Knob mutations from (12), where K1 is C3-G70, K2 is C10-G25, and K3 is G17. The boxed region on THG73 corresponds to the 2nd to 4th positions of the acceptor stem (mutations are shown in gray italics in the right box). Note THG73 K1 and TQAS-3 are the same mutation. Other tRNAs studied are shown at the bottom with only the 2nd to 4th positions of the acceptor stem shown. ENAS and TQAS contain the same nucleotides at these positions.

As shown in Figure 4.4, THG73 K2, THG73 K2K3, and THG73 K1K2K3 all show less than 20% aminoacylation *in vivo* when compared to THG73 at β9'UAG (Figure 4.4). However, when each tRNA was chemically ligated with dCA-W and injected with α149UAG (a non-permissive site), less than 3% of the current of THG73-W was seen (Figure 4.4). Therefore THG73 K2, THG73 K2K3, and THG73 K1K2K3 are nonfunctional in the *Xenopus* oocyte and are not viable alternatives for UAA incorporation *in vivo*.

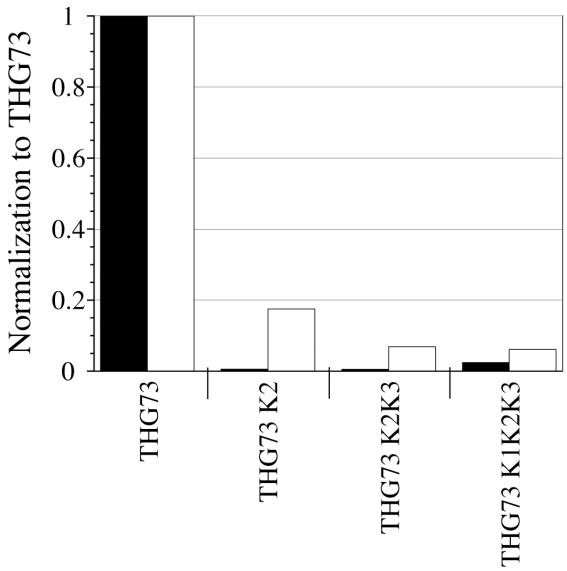

Figure 4.4: THG73 Knob mutations. Individual tRNA average current were normalized by appropriate THG73 average current and bars represent this average ratio. (Total number of oocytes tested is 91, where each bar is $15 > n > 5$ oocytes.) Black bars correspond to tRNA-W [21 ng per oocyte] suppressing at α149UAG and white bars correspond to tRNA (74mer) [17 ng per oocyte] + β9'UAG in Xenopus Express oocytes. THG73 Knob mutations are < 20% when suppressing at α149UAG and show they are not functional alternatives for UAA incorporation.

We conclude that THG73 is very sensitive to the K2 and K3 mutations in the D-stem and D-loop, respectively, which make tertiary contacts with the variable loop to form the characteristic L-shape, tRNA structure. Previous replacement of the THG73 anticodon with ACCC (8) and CCCG (3) also resulted in nonfunctional frameshift suppressors *in vivo*. THG73 appears to be exceptionally sensitive to mutation within the D domain and the anticodon loop, which limits the regions where this tRNA can be mutated to create functional tRNAs.

4.2.5 Testing Aminoacylation of ENAS and ENAS A71 *In Vivo*

With the failure of the knob mutations to produce functional tRNAs for UAA incorporation, we chose to screen the *E. coli* Asn amber suppressor (ENAS), which was shown to be orthogonal *in vitro* (4) and *in vivo* (9). When analyzing the structure of ENAS, we noticed that the 2nd position of the acceptor stem contained the non-Watson-Crick base pair U2-C71. We created the variant ENAS C71A to form the canonical pair U2-A71 (Figure 4.3) present in the wild-type tRNA (9).

While injection of ENAS or ENAS A71 (74mer) with β9'UAG resulted in less aminoacylation than THG73 in both Xenopus Express and Nasco oocytes, the effect was much more pronounced with Nasco oocytes (Figure 4.5). The EC_{50}s of ENAS (74mer) or ENAS A71 (74mer) with β9'UAG were 2.0 ± 0.1 and 1.5 ± 0.1 μM ACh, respectively, in Nasco oocytes. These EC_{50}s are larger than the 0.31 μM ACh for β9'Q (Figure 4.2), suggesting that ENAS and ENAS A71 are aminoacylated by another natural aa or a mixture of natural aas.

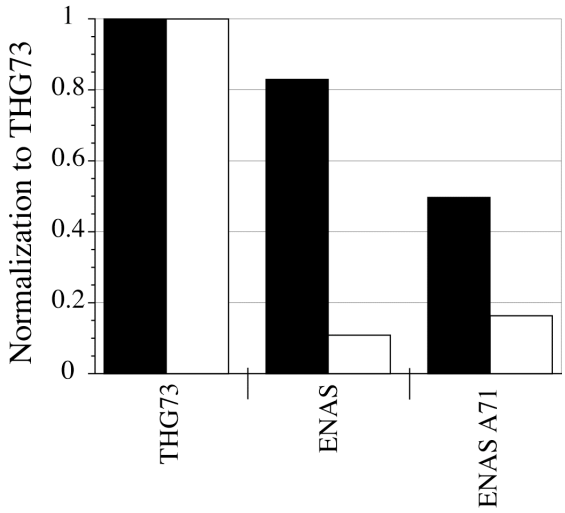

Figure 4.5: ENAS and ENAS A71 aminoacylation tested at β9'UAG. Individual tRNA (74mer) [17 ng per oocyte] average current was normalized to THG73 (74mer) average current and bars represent this average ratio. (Total number of oocytes tested is 75, where each bar is $22 > n > 5$ oocytes.) Black and white bars correspond oocytes from Xenopus Express and Nasco, respectively. ENAS and ENAS A71 show a large amount of aminoacylation in Xenopus Express oocytes after a 2 d incubation, which has not been seen *in vitro* (4) or *in vivo* (9). Aminoacylation is drastically reduced when tested in Nasco oocytes.

While ENAS and ENAS A71 tRNAs do show improved orthogonality compared to THG73, the suppression efficiencies of ENAS-W and ENAS A71-W were less than 26% of THG73-W in both Xenopus Express and Nasco oocytes (Chapter 5 & (23)). As such, neither ENAS tRNA is a viable replacement for THG73 for UAA incorporation in *Xenopus* oocytes.

4.2.6 Testing Aminoacylation of THG73 Acceptor Stem Mutations

The *E. coli* GlnRS contacts the tRNA acceptor stem in the crystal structure (13), and biochemical experiments have shown specific base pairs and/or positioning of the backbone affect aminoacylation *in vivo* (14–16). As such, we decided to screen various

mutations in the 2nd to 4th positions of the acceptor stem (shown in Figure 4.3) to create a library of *T. thermophila* Gln amber suppressor (TQAS) tRNAs (note in this nomenclature THG73 would be known as TQAS-0). The mutation G2C on THG73 (TQAS-1) results in the 2nd position having C2 C71, which results in a non-functional tRNA and serves as a negative control. The single helix pair mutations C2-G71, C3-G70, and C4 are named TQAS-2, TQAS-3, and TQAS-4, respectively (Figure 4.3). We then created the double helix pair mutation C3-G70 & C4 (TQAS-5) and the triple helix pair mutation C2-G71, C3-G70, & C4 (TQAS'). Finally we placed the ENAS acceptor stem from the 2nd to 4th position, including the U2-C71, on THG73 to create TQAS (Figure 4.3).

All acceptor stem mutations reduced aminoacylation relative to THG73 in both Xenopus Express and Nasco oocytes when tested at β9'UAG (Figure 4.6 & Table 4.1). TQAS-1 shows the same amount of current as β9'UAG mRNA injection alone, but due to the C2 C71 in the acceptor stem TQAS-1-W is unable to suppress α149UAG in both Xenopus Express and Nasco oocytes (Chapter 5 & (23)). In Xenopus Express oocytes, the single helix pair mutations on THG73 all lower aminoacylation, with orthogonality following the order TQAS-2 < TQAS-3 < TQAS-4 (Figure 4.6). Reduction is also seen for the single helix pair mutations in Nasco oocytes, but the orthogonality trend is TQAS-4 ≈ TQAS-3 < TQAS-2. These results are consistent with previous biochemistry experiments that showed the 2nd and 3rd positions are GlnRS identity elements (14,15),

and that removing the wobble (U4-G69) at the 4th position reduces aminoacylation in *E. coli* (16).

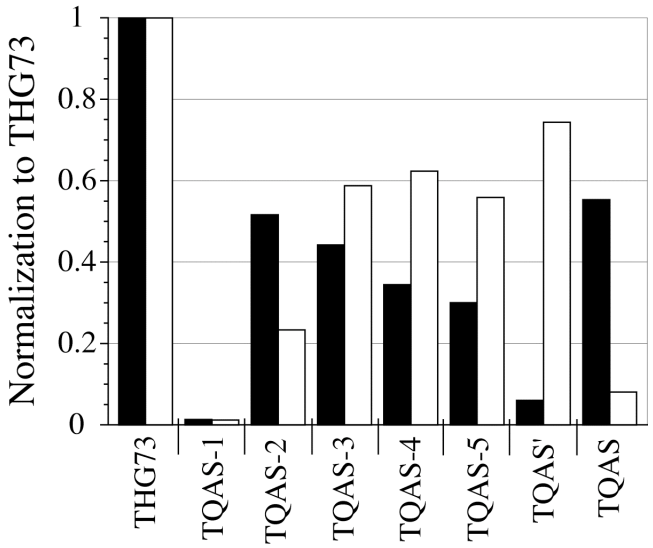

Figure 4.6: THG73 acceptor stem mutations tested at β9'UAG. Individual tRNA (74mer) [16 ng per oocyte] average current was normalized to THG73 (74mer) average current. Bar colors are the same as in Figure 4.5. Total number of oocytes tested is 189 and each bar is $26 > n > 8$ oocytes. All mutations in the acceptor stem lower aminoacylation *in vivo* relative to THG73. TQAS-1 shows lack of aminoacylation, but is not accepted by the translational machinery (Thesis Chapter 5 & (23)). TQAS' and TQAS are the most orthogonal tRNAs in Xenopus Express and Nasco oocytes, respectively.

Table 4.1: THG73 acceptor stem mutations

tRNA	Xenopus Express [a]	Nasco [a]	Average [b]
THG73	1.00	1.00	1.00
TQAS-1	0.01	0.01	0.01
TQAS-2	0.52	0.23	0.38
TQAS-3	0.44	0.59	0.52
TQAS-4	0.34	0.62	0.48
TQAS-5	0.30 (0.15) [c]	0.56	0.43
TQAS'	0.06 (0.08) [c]	0.74	0.40
TQAS	0.55	0.08	0.32
U2-C71 (TQAS)	*[4.27]* [d]	*[0.24]* [d]	*[1.43]* [d]

[a] Values from Figure 4.6.

[b] Average of Xenopus Express and Nasco aminoacylation from Figure 4.6.

[c] Theoretical values calculated by the multiplication of the single mutations.

[d] Theoretical value for U2-C71 calculated by TQAS/(TQAS-3 X TQAS-5).

We then combined mutations to reduce aminoacylation further in *Xenopus* oocytes. In Xenopus Express oocytes, combining the mutations results in a multiplicative reduction in aminoacylation for TQAS-5 and TQAS' (Table 4.1), while TQAS, which contains U2-C71, shows the largest amount of aminoacylation (Figure 4.6). The overall aminoacylation trend in Xenopus Express oocytes is THG73 >> TQAS ≈ TQAS-2 > TQAS-3 > TQAS-4 > TQAS-5 >> TQAS', making TQAS' the most orthogonal tRNA (Figure 4.6). The same tRNAs tested in Nasco oocytes show no logical trend in combining mutations (Table 4.1), and TQAS is the most orthogonal tRNA. Nasco oocytes display the overall aminoacylation trend THG73 >> TQAS' > TQAS-4 ≈ TQAS-3 ≈ TQAS-5 > TQAS-2 >> TQAS (Figure 4.6). Overall the mutations suggest C-G pairs in the acceptor stem reduce aminoacylation in Xenopus Express oocytes. Nasco oocytes prefer the C-G mutation at the 2nd position (TQAS-2, Figure

4.3) or the non-Watson-Crick U-C pair at the 2nd position, along with C-G pairs at the 3rd and 4th positions (TQAS, Figure 4.3). While differences in the Xenopus Express and Nasco oocytes were unanticipated, Figure 4.6 shows that the TQAS tRNA library contained an orthogonal tRNA for each genetic background.

4.2.7 Aminoacylation Tested at a Highly Promiscuous Site, βA70

The β9' site can incorporate many natural aas and UAAs (18–20), but we chose to further test aminoacylation of the orthogonal tRNAs selected (TQAS' and TQAS) at another highly permissive nAChR site, βA70. Structural studies place this residue on a highly exposed loop of the receptor (24,25). Previous work on the aligned αD70UAG showed that it can incorporate the large UAA biocytin with little change in the EC_{50} (26). Other work has shown that biocytin is a challenging residue for nonsense suppression (11), supporting the notion that αD70 is a promiscuous site. Therefore we studied the αD70-aligned site in the β-subunit, βA70, considering only Nasco oocytes.

With the injection of β70UAG mRNA only, large amounts of current were obtained, indicating that this read-through represents ≈ 30% of the current observed in the aminoacylation experiments (Figure 4.7). This large amount of read-through is not typical of most sites studied (β9'UAG discussed above and α145UAG below), and is most likely caused by the high promiscuity for aa incorporation. Injection of THG73-dCA and TQAS'-dCA with β70UAG in Nasco oocytes resulted in approximately the same amount of aminoacylation (Figure 4.7, white bars), which is consistent with increased TQAS' aminoacylation with Nasco oocytes (Figure 4.6). However, TQAS

shows very little aminoacylation compared to THG73 at this site (Figure 4.7), and subtracting the mRNA only results in 9% aminoacylation relative to THG73 (also background subtracted).

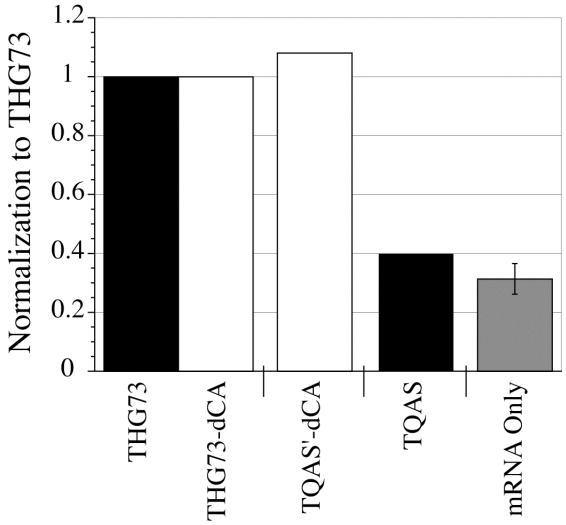

Figure 4.7: tRNA (74mer/-dCA) aminoacylation tested at a highly promiscuous site, βA70. All experiments were performed in Nasco oocytes. Black bars are tRNA (74mer), white bars are tRNA-dCA, and the gray bar is mRNA only. Average currents for TQAS'-dCA and TQAS were normalized to THG73-dCA and THG73, respectively. mRNA only was normalized to THG73. Total number of oocytes tested is 60, where each bar is $15 > n > 6$ oocytes with 9 ng of tRNA per oocyte. mRNA only shows significant read-through of the UAG stop codon. THG73, THG73-dCA, and TQAS'-dCA all show significant aminoacylation when assayed at β70UAG. TQAS shows comparable currents to the injection of mRNA only, showing less aminoacylation of TQAS in Nasco oocytes.

The EC_{50}s for mRNA only, THG73, TQAS'-dCA, and TQAS were 71 ± 1, 56 ± 3, 58 ± 3, and 46 ± 2 μM ACh, respectively, and showed little change from the wild-type EC_{50} of 50 μM ACh. These studies further show that TQAS is the most orthogonal tRNA and that TQAS' is aminoacylated extensively in Nasco oocytes.

4.2.8 LysRS Does Not Aminoacylate THG73, TQAS', and TQAS

THG73 was shown to be aminoacylated by Gln at the β9' site (Figure 4.2). However, the 9' position is a conserved Leu in all of the nAChR subunits and forms the hydrophobic gate to the channel (18). Therefore it is possible that anionic or cationic aas such as Asp, Glu, Lys, and Arg may not be incorporated at the β9' position or may produce nonfunctional receptors if they are. This is concerning because many amber suppressor tRNAs have been shown to be aminoacylated by LysRS and/or GlnRS *in vivo* (22), and mutations to the anticodon stem of an amber suppressor $tRNA^{Tyr}$ have shifted the GlnRS or LysRS recognition *in vitro* (27). To evaluate this possibility, we studied a conserved Lys residue in the α-subunit of the nAChR, αK145, to test if suppressor tRNAs were aminoacylated by LysRS and/or GlnRS. The conventional mutant αK145Q gave an EC_{50} of 144 ± 2 μM ACh (Figure 4.8), a ≈ 3-fold increase relative to the wild-type EC_{50} of 50 μM ACh.

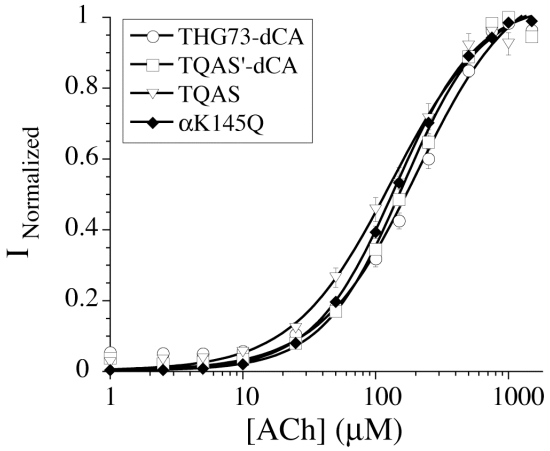

Figure 4.8: tRNA aminoacylation tested at αK145. Total number of oocytes tested is 36, where each dose-response is $17 > n > 5$ oocytes. EC_{50} values are 167 ± 14, 165 ± 14, 134 ± 15, and 144 ± 2 μM ACh in the order listed in the legend with 7.5 ng of tRNA per oocyte. All tRNAs are still aminoacylated by Gln and not Lys (wild-type EC_{50} = 50 μM ACh).

Injection of α145UAG mRNA alone resulted in very small currents, such that EC_{50} could not be determined. Injection of α145UAG with THG73-dCA, TQAS'-dCA, and TQAS resulted in EC_{50}s of 167 ± 14, 165 ± 14, and 134 ± 15 μM ACh, respectively (Figure 4.8). The EC_{50}s for all tRNAs are ≈ 3-fold increased relative to the wild-type EC_{50}, and therefore all of the tRNAs are aminoacylated by GlnRS and not by LysRS in *Xenopus* oocytes.

4.2.9 Analyzing THG73-W and TQAS-W Interactions with the Translational Machinery *In Vivo*

In Figure 4.1, we outlined the desired events for the incorporation of UAA and the undesired possibility of incorporation of natural aas at the suppression site. THG73 was previously shown to be orthogonal to the translational machinery *in vitro* and *in vivo* when using less mRNA and/or tRNA along with incubations less than 2 d (4–8). We

have shown that with increasing all three of the aforementioned conditions, producing so-called excessive conditions, THG73 can be aminoacylated *in vivo*. Under these same conditions, TQAS' shows ≈ 90% reduction in the aminoacylation product in Xenopus Express oocytes (Figure 4.6).

To analyze interactions with the translational machinery we used the temporal control of injection. By injecting tRNA-W first, we analyze the protection of the tRNA-W by EF-1α and/or other components of the translational machinery (Figure 4.1, A) from the undesired, irreversible loss of the UAA by hydrolysis and/or aaRS editing (Figure 4.1, C). Subsequent injection of mRNA to assay protein production (Figure 4.1, B) allows for comparison to what is seen when tRNA-W and mRNA are injected simultaneously. The tRNA-aa bond is highly labile at physiological pH. In a recent study, a sample of dCA-Val at pH 7.8 without translational machinery components was 69% hydrolyzed after a 1 h incubation (28). The cytoplasm of a *Xenopus* oocyte is estimated to be between pH 7.3–7.7 (29,30), and therefore some hydrolysis of tRNA-dCA-W would be expected after 3.5 h, if not protected by other proteins. EF-Tu has been shown to protect $YFFS_{CCCG}$-UAA from hydrolysis *in vitro*, but significant loss was seen after 1 h (17).

Simultaneous injection of THG73-W/TQAS'-W (10 ng per oocyte) and α149UAG mRNA gave average maximal currents of -3.9 ± 1 and -4.1 ± 1 μA, respectively, in Xenopus Express oocytes. Surprisingly, we see no loss in current from either THG73-W or TQAS'-W when injecting mRNA 3.5 h after the tRNA-W, with -3.9

± 0.5 and -3.9 ± 1 μA, respectively. Injection of twice as much THG73-W (20 ng per oocyte) resulted in -6.3 ± 2 μA. This illustrates that the translation system is not saturated, but there is not a linear increase in current with twice as much tRNA-W in a single injection. Therefore, interactions with EF-1α and/or other proteins specifically protect both suppressor tRNA-Ws from deacylation by aaRS(s) and hydrolysis, which is not problematic after 3.5 h in the *Xenopus* oocytes.

A double injection protocol, in which a second dose of aminoacyl tRNA is injected 24 h after the first, allows us to assay competition between the suppressor tRNA-W and tRNA-Q (generated by aminoacylation *in vivo*) after 24 h (Figure 4.1, B & G). Only aromatic aas can function at α149UAG, and suppressing with tRNA-W results in wild-type channels. If, however, there is competition with tRNA-Q, then, during the second 24 h there will be a decrease in the overall protein production, or less than double the current. In the event, a double injection with a 24 h interval of THG73-W/TQAS'-W with α149UAG showed currents of -8.9 ± 2 and -8.6 ± 3 μA, respectively, which is greater than twice the protein relative to the single injection. The higher protein production is mostly likely due to residual mRNA from the 1st injection, even though nonsense-mediated decay in *Xenopus* oocytes is expected to remove most mRNA with premature stop codons after 18 h (31).

The double injection studies establish that aminoacylation of the tRNA-dCA in Xenopus oocytes (Figure 4.1, E–H) is not problematic for the first 24+ h *in vivo* for either THG73 and TQAS', because there is no reduction in protein and therefore lack of

competition for the suppression site. This is surprising because THG73 is aminoacylated ≈ 90% more than TQAS' in Xenopus Express oocytes after 2 d (Figure 4.6). This does, however, agree with previous investigations of THG73 orthogonality *in vivo* with incubations of 24 h or less (7).

4.2.10 Comparing Aminoacylation of Amber, Opal, and Frameshift Suppressor tRNAs

Increasing the number of UAAs to be simultaneously incorporated site-specifically requires the use of a unique stop or quadruplet codon for each UAA. Previously we screened two yeast Phe frameshift suppressor tRNAs, $YFFS_{CCCG}$ and $YFaFS_{ACCC}$, in *Xenopus* oocytes and found that both tRNAs were aminoacylated much less than THG73 when tested at the β9' site. However, their suppression efficiency was decreased relative to THG73 *in vivo*, although still adequate for UAA incorporation (3). Previous work has established that the opal (UGA) and ochre (UAA) stop codons can be suppressed in mammalian cells when using suppressor tRNAs that are aminoacylated by endogenous aaRSs (32) or by the import of an exogenous *E. coli* aaRSs (33). The opal codon has also been used to incorporate an UAA in mammalian cells using a tRNA/synthetase pair (34). Also, an opal suppressor was previously created by replacing the anticodon of THG73 with UCA, but this opal suppressor tRNA (not chemically ligated to an UAA) is aminoacylated *in vitro* and results in protein translation, or aminoacylation product, > 90% when compared to wild-type translation. Under the same conditions as the opal suppressor tRNA, THG73 and ENAS showed < 5%

aminoacylation product (4), suggesting that the opal suppressor derived from THG73 would be highly aminoacylated *in vivo* and not viable for nonsense suppression. In *T. thermophila*, the ochre suppressor has been shown to suppress both the ochre and amber codons (21), and so it would not be viable for the simultaneous incorporation of multiple UAAs.

To test the generality of the acceptor stem mutations at reducing aminoacylation *in vivo*, we created *T. thermophila* Gln opal suppressor tRNAs (TQOpS' and TQOpS) by replacing the anticodon of TQAS' and TQAS with UCA.

All four subunits of the nAChR terminated with the opal (UGA) stop codon, and these were all mutated to the ochre (UAA) stop codon to avoid suppression by TQOpS' or TQOpS. The masked construct had an EC_{50} of 53 ± 3 μM ACh, comparable to the wild-type EC_{50} of 50 μM. Injection of β9'UGA with no tRNA resulted in 2.8% of the current normalized to THG73 (74mer), vs. 1.7% with β9'UAG. The opal codon thus showed ≈ 1.6-fold greater read-through than the amber codon, which has previously been noted in *E. coli* (35). Aminoacylation was tested under identical conditions with THG73, TQAS', TQAS, TQOpS', TQOpS, $YFFS_{CCCG}$, and $YFaFS_{ACCC}$ at the β9' suppression site, stop codon or quadruplet codon, with tRNA (74mer) and tRNA-dCA (76mer). This was done to validate initial screens using only (74mer) and comparisons between (74mer) and (76mer) in Figures 4.4, 4.5, 4.6, and 4.7. Comparison of suppressor tRNAs (74mer) and tRNA-dCAs (76mer) show no significant difference for each individual suppressor tRNA in Xenopus Express or Nasco oocytes (Figure 4.9).

Once again TQAS' and TQAS showed much less aminoacylation in Xenopus Express and Nasco oocytes, respectively, relative to THG73. TQOpS' and TQOpS both show less than ≈ 40% and ≈ 9% aminoacylation, respectively, compared to THG73 (Figure 4.9). This shows that the acceptor stem mutations on THG73 are able to reduce aminoacylation for both amber and opal suppressor tRNAs. $YFaFS_{ACCC}$ and $YFFS_{CCCG}$ show a similar trend to that previously reported (Chapter 3 & (3)) with average aminoacylation product of 19% and 3%, respectively, of THG73. The orthogonality trend is as follows: $YFaFS_{ACCC}$ > TQAS' (Xenopus Express) ≈ TQOpS > $YFFS_{CCCG}$ > TQAS (Nasco) ≈ TQOpS' >> THG73, which is aminoacylated the most.

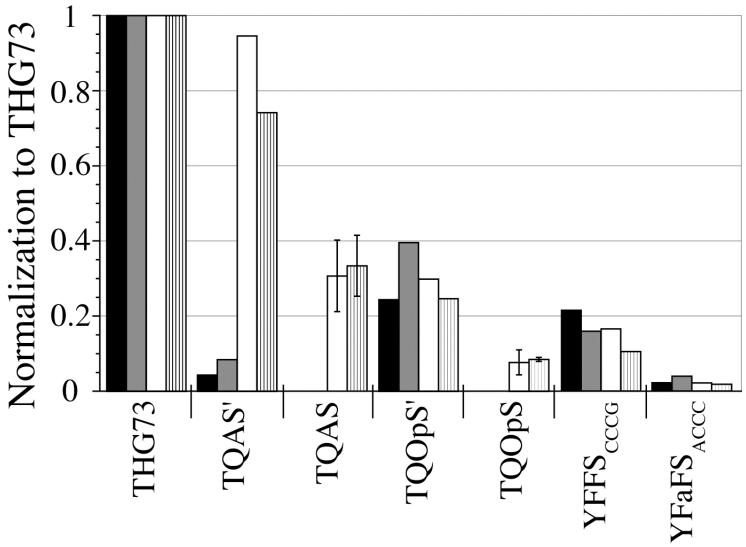

Figure 4.9: Amber, opal, and frameshift suppressor tRNAs tested at β9'. All tRNA 74mer or -dCA [7.5 ng per oocyte] average currents were normalized to THG73 74mer or -dCA average currents, respectively. Black bars are tRNA 74mer + β9'(UAG, UGA, CGGG, or GGGU) and gray bars are tRNA-dCA (76mer) + β9'(UAG, UGA, CGGG, or GGGU) in Xenopus Express oocytes. White and Hatched bars are tRNA 74mer and 76mer, respectively, in Nasco oocytes. Total number of oocytes is 276, where $17 > n > 5$. TQAS' and TQAS show significantly reduced aminoacylation in Xenopus Express and Nasco oocytes, respectively, when compared to THG73. Both opal suppressor tRNAs (TQOpS' and TQOpS) show less aminoacylation than THG73. Overall, the frameshift suppressor YFaFS$_{ACCC}$ is the most orthogonal tRNA in both Xenopus Express and Nasco oocytes.

4.3 Discussion

THG73 is an amber suppressor tRNA that has been used extensively for the incorporation of greater than 100 residues in 20 proteins (1,2). Using conditions such as low quantities of mRNA and/or tRNA with incubation times less than 2 d, THG73 has been shown to be orthogonal *in vitro* (4–6) and *in vivo* (7,8). However, increasing the amount of mRNA and tRNA with incubation of 2 d leads to the aminoacylation of THG73 by an endogenous aaRS *in vivo* (3). We show that the *E. coli* Asn amber

suppressor (ENAS) and ENAS A71 are both susceptible to aminoacylation by aaRSs of the *Xenopus* oocyte (Figure 4.5), even though aminoacylation has not been observed *in vitro* (4,10,11) or *in vivo* (9). This suggests that many well-characterized amber suppressor tRNAs may become aminoacylated *in vivo* when using increased amounts of mRNA and tRNA along with incubations of 2 d, which is desirable for increased amounts of protein.

By using the sensitivity of electrophysiology and the well-characterized β9' site, we have been able to show that the natural aa placed on THG73 is predominantly if not exclusively Gln (Figure 4.2). The THG73 (74mer) and β9'Q show comparable EC_{50}s, but THG73-dCA (76mer) shows ≈ 3-fold increase in EC_{50} (Figure 4.2). These experiments suggest that THG73-dCA (76mer) is more readily aminoacylated by other endogenous aaRSs, perhaps due to the unnatural dCA at the 3' end, but the predominant aa is still Gln. Similar conditions with the THG73 (74mer) resulted in equivalent EC_{50} as β9'Q and therefore the active THG73-CA (Figure 4.1, D) appears to be more stringently recognized by the GlnRS.

Intriguingly, THG73 is very sensitive to the previously discussed "knob" mutations meant to disrupt recognition by GlnRS, and the derived tRNAs are not viable for UAA incorporation. The K2 mutation alone destroys activity, and combining it with other knob mutations provides little rescue. The K2 mutation resides within the D domain of THG73, which makes tertiary contacts with the variable loop to form the characteristic L-shape tRNA structure. This mutation may result in misfolding of the

THG73, but it apparently has little effect on *E. coli* $tRNA_2^{Gln}$ (12). Interestingly, the K1, or TQAS-3, mutation was shown to be functional by itself on THG73 (Chapter 5 & (23)), but it is non-functional in combination with K2 and K3 (Figure 4.4). Replacement of the THG73 anticodon with ACCC (8) or CCCG (3) resulted in nonfunctional frameshift suppressors *in vivo*. THG73 appears to be sensitive to mutation within the D domain and the anticodon loop, but tolerates acceptor stem mutations.

ENAS and ENAS A71 aminoacylation in Xenopus Express oocytes is comparable to THG73, but there is a 40% decrease due to the U2-C71 vs. U2-A71, respectively, (Figure 4.5) at the 2nd position of the acceptor stem (Figure 4.3). ENAS A71 is more orthogonal, which suggests that the U-A is not recognized by endogenous aaRSs as readily as U-C. The opposite trend is seen in Nasco oocytes, but orthogonality is significantly improved for both ENAS and ENAS A71. Clearly, the identity of the 2nd pair has a strong effect on aminoacylation *in vivo*.

We hypothesized that similar mutations on THG73 could result in less aminoacylation by the GlnRS, because the identity set includes the 2nd to 4th positions of the acceptor stem (13–16). The acceptor stem mutations (shown in Figure 4.3) greatly reduced aminoacylation *in vivo* (Figure 4.6 & Table 4.1). In Xenopus Express oocytes, the single helix pair mutations could be combined to further reduce aminoacylation in a multiplicative manner (Table 4.1). In contrast, Nasco oocytes showed a strong dependence on specific sequences, and there was no logical trend based on the single helix pair mutations. This non-classical identity set has previously been identified on

yeast Phe tRNA, where combining mutations could compensate for deleterious single mutations to increase aminoacylation *in vitro* (36). While variation due to the Xenopus Express and Nasco oocytes was unanticipated, the library of six functional TQAS tRNAs was able to find an orthogonal suppressor tRNA for each genetic background. We can anticipate that as other workers move the UAA methodology into other cell types, different orthogonality issues could arise. The library of tRNAs created here contains diverse mutations in the acceptor stem that should allow for orthogonal tRNA selection in other eukaryotic cells, where high-throughput assays for tRNA screening are currently lacking.

Using the temporal control of injection, we were able to evaluate THG73-W and TQAS'-W interactions with the protein translation machinery and competition with the suppressor tRNAs aminoacylated with Gln after 1 d. Shockingly, there is no change in suppression efficiency when the mRNA and tRNA-W are injected simultaneously or when the mRNA was injected 3.5 h after tRNA-W. These experiments show that both suppressor tRNAs are equally protected by EF-1α and/or other components of the translational machinery for at least 3.5 h, which has not been observed *in vitro* with or without EF-Tu (17,28). Most importantly, this shows that aaRS editing and/or hydrolysis (Figure 4.1, C) are not problematic with 10 ng of tRNA-W injected in oocytes. Injection of 20 ng of THG73-W resulted in a 60% increase in current with a single injection, establishing the lack of saturation at 10 ng, although the response is non-linear. By injecting mRNA and tRNA-W followed by a 2nd injection of the same after

24 h, we could see if there was competition for the suppression of α149UAG by tRNA-Q (Figure 4.1, B & G). The double injection for both THG73-W/TQAS'-W showed a slightly greater than 2-fold increase in current, indicating a lack of competition with tRNA-Q slightly after 24 h. This agrees with previous experiments using less than 24 h incubation times (7,8). Aminoacylation of THG73 therefore takes place after 24 h and is not different from TQAS' in Xenopus Express oocytes in the first 24 h. However, TQAS' is aminoacylated ≈ 90% less than THG73 after 2 d. Overall, both THG73 and TQAS' interact with the protein translational machinery similarly in Xenopus Express oocytes.

In order to simultaneously incorporate multiple UAAs, it is necessary to use a unique stop or quadruplet codon for each UAA. Previously, three UAAs could be simultaneously incorporated using amber and frameshift suppression with the UAG, CGGG, and GGGU suppression sites (3). A second nonsense site, either opal (UGA) or ochre (UAA), would be valuable for the incorporation of four UAAs. However, the *T. thermophila* ochre suppressor recognizes both the ochre (UAA) and amber (UAG) stop codons (21). The opal codon has been used to incorporate an UAA in mammalian cells using a tRNA/synthetase pair (34) and should be feasible for the UAA incorporation in *Xenopus* oocytes. Previous work with an opal suppressor created from THG73 by the replacement of the anticodon with UCA resulted in a large amount of aminoacylation *in vitro* and production of greater than 90% protein relative to wild-type protein (4). These results suggest that the THG73-derived opal suppressor would be aminoacylated much

more than the THG73 amber suppressor and would not be able to be evaluated under the conditions tested in this paper. To test the generality of the acceptor stem mutations at reducing aminoacylation, we replaced the anticodon of TQAS' and TQAS with UCA to create TQOpS' and TQOpS, respectively. Both TQOpS' and TQOpS show a great reduction in aminoacylation *in vivo* relative to THG73 (Figure 4.9) and are viable suppressor tRNAs for UAA incorporation at the opal codon (Chapter 5 & (23)). Intriguingly, there is no significant difference in aminoacylation of TQOpS' in Xenopus Express and Nasco oocytes (Figure 4.9), which suggests the opal suppressor is recognized by a different aaRS(s) and variation in aminoacylation is caused by the GlnRS, which we have shown recognizes THG73, TQAS', and TQAS (Figure 4.8); the tRNAs show different amounts of aminoacylation depending on the genetic background (Figures 4.6 & 4.9).

We have shown that acceptor stem mutations have wide applicability for the creation of orthogonal suppressor tRNAs for the incorporation of UAAs in higher eukaryotic cells. TQAS' and TQAS still retain slight aminoacylation by the GlnRS in Xenopus Express and Nasco oocytes, respectively. Mutations in the anticodon stem have been shown to decrease GlnRS recognition and may further reduce aminoacylation, but these mutations can also lead to increased LysRS recognition (27). The acceptor stem mutations have no adverse effect on the suppression efficiency and can increase the suppression efficiency by as much as 40% (Chapter 5 & (23)). While aminoacylation

was shown to be dependent on the genetic background of the oocytes, there is no effect on the suppression efficiencies of the TQAS tRNAs (Chapter 5 & (23)).

In summary, we have created a TQAS tRNA library that will aid in the identification of orthogonal tRNAs for use with higher eukaryotic cells. When combined with the evaluation of suppression efficiencies described in Chapter 5 and (23), these tRNAs should significantly expand the applicability of site-specific incorporation of UAAs by chemically aminoacylated tRNAs.

4.4 Experimental Methods

4.4.1 Materials

All oligonucleotides were synthesized by Integrated DNA Technologies (Coralville, IA). NotI was from Roche Applied Science (Indianapolis). BamHI, EcoRI, FokI, T4 DNA ligase, and T4 RNA ligase were from NEB (Beverly, MA). Kinase Max, T7 MEGAshortscript, and T7 mMessage mMachine kits were from Ambion (Austin, TX). ACh chloride and yeast inorganic pyrophosphatase were purchased from Sigma-Aldrich. dCA and 6-nitroveratryloxycarbonyl protected dCA-W was prepared as reported in (37,38).

4.4.2 tRNA Gene Preparation and tRNA Transcription

THG73, $YFFS_{CCCG}$, and $YFaFS_{ACCC}$ subcloned in the pUC19 vector were previously made (3,7). Genes for ENAS (sequence from (4)) with flanking EcoRI and BamHI overhangs were phosphorylated using Kinase Max kit, annealed, and ligated with

T4 DNA ligase into EcoRI and BamHI linearized pUC19 vector as described (39). ENAS A71 (original sequence from (9) with G1-C72 insertion for T7 polymerase transcription) was created by QuikChange mutagenesis on ENAS in pUC19. Knob mutations from (12) (K2 is C10-G25; K2K3 is C10-G25 & G17; and K1K2K3 is C3-G70, C10-G25, & G17) on THG73 were created by QuikChange mutagenesis. Acceptor stem mutations on THG73 were created by QuikChange mutagenesis and shown in Figure 4.3. Replacing the anticodon of TQAS' and TQAS from CUA to UCA by QuikChange mutagenesis created TQOpS' and TQOpS, respectively. All mutations were verified by DNA sequencing (California Institute of Technology Sequencing / Structure Analysis Facility). Template DNA for tRNA lacking the 3'CA was prepared by FokI digestion, and tRNA was transcribed using the T7 MEGAshortscript kit with .5 μl of yeast inorganic pyrophosphatase (40 U/ml in 75 mM Tris, 10 mM $MgCl_2$, and pH 7). tRNA was desalted using CHROMA SPIN-30 DEPC-H_2O columns (BD Biosciences), and concentration was determined by absorption at 260 nm.

4.4.3 nAChR Gene Preparation and mRNA Transcription

The masked α-, β-, γ-, and δ-subunits of the nAChR subcloned in the pAMV vector were previously prepared (3). All four subunits terminate with the opal (UGA) stop codon and each UGA was mutated to the ochre (UAA) stop codon to avoid possible suppression by TQOpS' and TQOpS. α149UAG and β9'(UAG, CGGG, and GGGU) were previously prepared on the masked constructs (3). β70UAG, α145Q, α145UAG, and β9'UGA were prepared by QuikChange mutagenesis. Mutations were verified by

DNA sequencing (California Institute of Technology Sequencing / Structure Analysis Facility). DNA was linearized with NotI and mRNA was prepared with the T7 mMessage mMachine kit with .5 μl of yeast inorganic pyrophosphatase. mRNA was purified by using the RNeasy Mini kit (Qiagen, Valencia, CA) and quantified by absorption at 260 nm.

4.4.4 dCA and dCA-W Ligation to Suppressor tRNAs

75 μM (used instead of 300 μM because there was no change in ligation efficiency) of dCA or 6-nitroveratryloxycarbonyl protected dCA-W were coupled to suppressor tRNAs by using T4 RNA ligase for 30 min as previously reported (39,40), desalted using CHROMA SPIN-30 DEPC-H_2O columns, and quantified by absorption at 260 nm. tRNA ligation efficiency was qualitatively determined by MALDI mass spectrometry (40), and all tRNA ligations were identical within each prepared group and greater than 80%.

4.4.5 *In Vivo* Aminoacylation and Suppression Experiments

Prior to *in vivo* aminoacylation and suppression experiments, all tRNAs and mRNAs were simultaneously made and normalized by UV and densiometric analysis using AlphaEaseFC Stand Alone (Alpha Innotech, San Leandro, CA). Stage VI oocytes of *Xenopus laevis* were prepared as described (41). All tRNAs were refolded at 65 ˚C for 2 min and 6-nitroveratryloxycarbonyl protected dCA-W was deprotected for 5 min by UV irradiation before injection (7). Oocytes were injected with 50 nl of mRNA alone or with tRNA and incubated at 18 ˚C for 44–52 h. For EC_{50} determination of β9'Q

(Figure 4.2), 3 ng of mRNA in the ratio of 2:1:1:1 for α:β9'Q:γ:δ was injected. 20 ng of mRNA in a subunit ratio of 2:5:1:1 for α:β9'UAG:γ:δ or 10:1:1:1 for α149UAG:β:γ:δ was injected in Figures 4.2, 4.4, and 4.5. Figures 4.6, 4.7, and 4.8 used the same ratio, but 40 ng to 60 ng of mRNA was injected per oocyte. In Figure 4.9, 40 ng of mRNA was injected in a subunit ratio of 2:5:1:1 for α:β9'(UAG, UGA, CGGG, or GGGU):γ:δ. The amount of tRNA injected is listed with each figure.

4.4.6 Electrophysiology

Recordings employed two-electrode voltage clamp on the OpusXpress 6000A (Molecular Devices). ACh was stored at -20 ˚C as a 1 M stock, diluted in Ca^{2+}-free ND96, and delivered to oocytes by computer-controlled perfusion system. For all experiments, the holding potential was -60 mV. Dose-response data was obtained from at least eight ACh concentrations and all tRNA aminoacylation or suppression comparisons were tested with a single 1 mM ACh dose. Dose-response relations were fit to the Hill equation to determine the EC_{50} and Hill coefficient (n_H). All reported values are represented as a mean ± SE of the tested oocytes (number of oocytes (n) is listed with each figure).

4.5 References

1. Dougherty, D.A. (2000) Unnatural amino acids as probes of protein structure and function. *Curr. Opin. Biotechnol.*, **4**, 645–652.

2. Beene, D.L., Dougherty, D.A., and Lester, H.A. (2003) Unnatural amino acid mutagenesis in mapping ion channel function. *Curr. Opin. Neurobiol.*, **13**, 264–270.

3. Rodriguez, E.A., Lester, H.A., and Dougherty, D.A. (2006) *In vivo* incorporation of multiple unnatural amino acids through nonsense and frameshift suppression. *Proc. Natl. Acad. Sci. USA*, **103**, 8650–8655.

4. Cload, S.T., Liu, D.R., Froland, W.A., and Schultz, P.G. (1996) Development of improved tRNAs for *in vitro* biosynthesis of proteins containing unnatural amino acids. *Chem. Biol.*, **3**, 1033–1038.

5. England, P.M., Lester, H.A., and Dougherty, D.A. (1999) Mapping disulfide connectivity using backbone ester hydrolysis. *Biochemistry*, **38**, 14409–14415.

6. Rothman, D.M., Petersson, E.J., Vazquez, M.E., Brandt, G.S., Dougherty, D.A., and Imperiali, B. (2005) Caged phosphoproteins. *J. Am. Chem. Soc.*, **127**, 846–847.

7. Saks, M.E., Sampson, J.R., Nowak, M.W., Kearney, P.C., Du, F.Y., Abelson, J.N., Lester, H.A., and Dougherty, D.A. (1996) An engineered *Tetrahymena* $tRNA^{Gln}$ for *in vivo* incorporation of unnatural amino acids into proteins by nonsense suppression. *J. Biol. Chem.*, **271**, 23169–23175.

8. Shafer, A.M., Kalai, T., Bin Liu, S.Q., Hideg, K., and Voss, J.C. (2004) Site-specific insertion of spin-labeled L-amino acids in *Xenopus* oocytes. *Biochemistry*, **43**, 8470–8482.

9. Kleina, L.G., Masson, J.M., Normanly, J., Abelson, J., and Miller, J.H. (1990) Construction of *Escherichia coli* amber suppressor tRNA genes. II. Synthesis of additional tRNA genes and improvement of suppressor efficiency. *J. Mol. Biol.*, **213**, 705–717.

10. Murakami, H., Kourouklis, D., and Suga, H. (2003) Using a solid-phase ribozyme aminoacylation system to reprogram the genetic code. *Chem. Biol.*, **10**, 1077–1084.

11. Murakami, H., Ohta, A., Ashigai, H., and Suga, H. (2006) A highly flexible tRNA acylation method for non-natural polypeptide synthesis. *Nat. Methods*, **3**, 357–359.

12. Liu, D.R., Magliery, T.J., and Schultz, P.G. (1997) Characterization of an 'orthogonal' suppressor tRNA derived from *E. coli* $tRNA_2^{Gln}$. *Chem. Biol.*, **4**, 685–691.

13. Perona, J.J., Swanson, R.N., Rould, M.A., Steitz, T.A., and Soll, D. (1989) Structural basis for misaminoacylation by mutant *E. coli* glutaminyl-tRNA synthetase enzymes. *Science*, **246**, 1152–1154.

14. Jahn, M., Rogers, M.J., and Soll, D. (1991) Anticodon and acceptor stem nucleotides in $tRNA^{Gln}$ are major recognition elements for *E. coli* glutaminyl-tRNA synthetase. *Nature*, **352**, 258–260.

15. Ibba, M., Hong, K.W., Sherman, J.M., Sever, S., and Soll, D. (1996) Interactions between tRNA identity nucleotides and their recognition sites in glutaminyl-tRNA synthetase determine the cognate amino acid affinity of the enzyme. *Proc. Natl. Acad. Sci.*, **93**, 6953–6958.

16. McClain, W.H., Schneider, J., Bhattacharya, S., and Gabriel, K. (1998) The importance of tRNA backbone-mediated interactions with synthetase for aminoacylation. *Proc. Natl. Acad. Sci.*, **95**, 460–465.

17. Nakata, H., Ohtsuki, T., Abe, R., Hohsaka, T., and Sisido, M. (2006) Binding efficiency of elongation factor Tu to tRNAs charged with nonnatural fluorescent amino acids. *Anal. Biochem.*, **348**, 321–323.

18. Kearney, P.C., Zhang, H., Zhong, W., Dougherty, D.A., and Lester, H.A. (1996) Determinants of nicotinic receptor gating in natural and unnatural side chain structures at the M2 9' position. *Neuron*, **17**, 1221–1229.

19. Filatov, G.N., and White, M.M. (1995) The role of conserved leucines in the M2 domain of the acetylcholine receptor in channel gating. *Mol. Pharmacol.*, **48**, 379–384.

20. Kosolapov, A.V., Filatov, G.N., and White, M.M. (2000) Acetylcholine receptor gating is influenced by the polarity of amino acids at position 9' in the M2 domain. *J. Membr. Biol.*, **174**, 191–197.

21. Hanyu, N., Kuchino, Y., Nishimura, S., and Beier, H. (1986) Dramatic events in ciliate evolution: Alteration of UAA and UAG termination codons to glutamine codons due to anticodon mutations in two *Tetrahymena* $tRNAs^{Gln}$. *EMBO. J.*, **5**, 1307–1311.

22. Normanly, J., Kleina, L.G., Masson, J.M., Abelson, J., and Miller, J.H. (1990) Construction of *Escherichia coli* amber suppressor tRNA genes. III. Determination of tRNA specificity. *J. Mol. Biol.*, **213**, 719–726.

23. Rodriguez, E.A., Lester, H.A., and Dougherty, D.A. (2007) Improved amber and opal suppressor tRNAs for incorporation of unnatural amino acids *in vivo*. Part 2: Evaluating suppression efficiency. *RNA*, **13**, 1715–1722.

24. Unwin, N. (2005) Refined structure of the nicotinic acetylcholine receptor at 4Å resolution. *J. Mol. Biol.*, **346**, 967–989.

25. Brejc, K., van Dijk, W.J., Klaassen, R.V., Schuurmans, M., van Der Oost, J., Smit, A.B., and Sixma, T.K. (2001) Crystal structure of an ACh-binding protein reveals the ligand-binding domain of nicotinic receptors. *Nature*, **411**, 269–276.

26. Gallivan, J.P., Lester, H.A., and Dougherty, D.A. (1997) Site-specific incorporation of biotinylated amino acids to identify surface-exposed residues in integral membrane proteins. *Chem. Biol.*, **4**, 739–749.

27. Fukunaga, J., Ohno, S., Nishikawa, K., and Yokogawa, T. (2006) A base pair at the bottom of the anticodon stem is reciprocally preferred for discrimination of cognate tRNAs by *Escherichia coli l*ysyl- and glutaminyl-tRNA synthetases. *Nucleic Acids Res*., **34**, 3181–3188.

28. Wang, B., Zhou, J., Lodder, M., Anderson, R.D., 3rd, and Hecht, S.M. (2006) Tandemly activated tRNAs as participants in protein synthesis. *J. Biol. Chem*., **281**, 13865–13868.

29. Webb, D.J., and Nuccitelli, R. (1981) Direct measurement of intracellular pH changes in *Xenopus* eggs at fertilization and cleavage. *J. Cell. Biol*., **91**, 562–567.

30. Sasaki, S., Ishibashi, K., Nagai, T., and Marumo, F. (1992) Regulation mechanisms of intracellular pH of *Xenopus laevis* oocyte. *Biochim. Biophys. Acta*., **1137**, 45–51.

31. Whitfield, T.T., Sharpe, C.R., and Wylie, C.C. (1994) Nonsense-mediated mRNA decay in *Xenopus* oocytes and embryos. *Dev. Biol*., **165**, 731–734.

32. Capone, J.P., Sedivy, J.M., Sharp, P.A., and RajBhandary, U.L. (1986) Introduction of UAG, UAA, and UGA nonsense mutations at a specific site in the *Escherichia coli* chloramphenicol acetyltransferase gene: use in measurement of amber, ochre, and opal suppression in mammalian cells. *Mol. Cell. Biol*., **6**, 3059–3067.

33. Kohrer, C., Sullivan, E.L., and RajBhandary, U.L. (2004) Complete set of orthogonal 21st aminoacyl-tRNA synthetase-amber, ochre and opal suppressor

tRNA pairs: concomitant suppression of three different termination codons in an mRNA in mammalian cells. *Nucleic Acids Res.*, **32**, 6200–6211.

34. Zhang, Z., Alfonta, L., Tian, F., Bursulaya, B., Uryu, S., King, D.S., and Schultz, P.G. (2004) Selective incorporation of 5-hydroxytryptophan into proteins in mammalian cells. *Proc. Natl. Acad. Sci. USA*, **101**, 8882–8887.

35. Anderson, J.C., and Schultz, P.G. (2003) Adaptation of an orthogonal archaeal leucyl-tRNA and synthetase pair for four-base, amber, and opal suppression. *Biochemistry*, **42**, 9598–9608.

36. Frugier, M., Helm, M., Felden, B., Giege, R., and Florentz, C. (1998) Sequences outside recognition sets are not neutral for tRNA aminoacylation. Evidence for nonpermissive combinations of nucleotides in the acceptor stem of yeast $tRNA^{Phe}$. *J. Biol. Chem.*, **273**, 11605–11610.

37. Robertson, S.A., Noren, C.J., Anthony-Cahill, S.J., Griffith, M.C., and Schultz, P.G. (1989) The use of 5'-phospho-2 deoxyribocytidylylriboadenosine as a facile route to chemical aminoacylation of tRNA. *Nucleic Acids Res.*, **17**, 9649–9660.

38. Zhong, W., Gallivan, J.P., Zhang, Y., Li, L., Lester, H.A., and Dougherty, D.A. (1998) From ab initio quantum mechanics to molecular neurobiology: A cation-π binding site in the nicotinic receptor. *Proc. Natl. Acad. Sci. USA*, **95**, 12088–12093.

39. Nowak, M.W., Gallivan, J.P., Silverman, S.K., Labarca, C.G., Dougherty, D.A., and Lester, H.A. (1998) *In vivo* incorporation of unnatural amino acids into ion channels in *Xenopus* oocyte expression system. *Meth. Enzymol.*, **293**, 504–529.

40. Petersson, E.J., Shahgholi, M., Lester, H.A., and Dougherty, D.A. (2002) MALDI-TOF mass spectrometry methods for evaluation of *in vitro* aminoacyl tRNA production. *RNA*, **8**, 542–547.

41. Quick, M.W., and Lester, H.A. (1994) Methods for expression of excitability proteins in *Xenopus* oocytes. In Narahashi, T. (ed.), *Ion Channels of Excitable Cells*. Academic Press, San Diego, CA, Vol. 19, pp. 261–279.